

Cylindrical Zwitterionic Particles via Interpolyelectrolyte Complexation on Molecular Polymer Brushes

*Th ophile Pelras, Nonappa, Clare S. Mahon and Markus M llner**

Dr. T. Pelras, Dr. M. M llner

Key Centre for Polymers and Colloids, School of Chemistry and Sydney Nano, The University of Sydney, NSW 2006, Australia.

E-mail: markus.muellner@sydney.edu.au

Dr. Nonappa

Faculty of Engineering and Natural Sciences, Tampere University, FI-33101 Tampere, Finland.

Dr. C.S. Mahon

Department of Chemistry, Durham University, DH1 3LE, The United-Kingdom.

Keywords: bottlebrushes, block copolymers, self-assembly, polyplex, template chemistry

Abstract

The fabrication of macromolecular architectures with high aspect ratio and well-defined internal and external morphology remains a challenge. The combination of template chemistry and self-assembly concepts to construct peculiar polymer architectures via a bottom-up approach is an emerging approach. In this study, a cylindrical template – namely a core-shell molecular polymer brush – and linear diblock copolymers associate to produce high aspect ratio polymer particles via interpolyelectrolyte complexation. Induced morphological changes are studied using cryogenic transmission electron and atomic force microscopy, while the complexation is further followed by isothermal titration calorimetry and ξ -potential measurements. Depending on the nature of the complexing diblock copolymer, distinct morphological differences can be achieved. While polymers with a non-ionic block lead to internal compartmentalisation, polymers featuring zwitterionic domains lead to a homogenous wrapping of the brush template.

Introduction

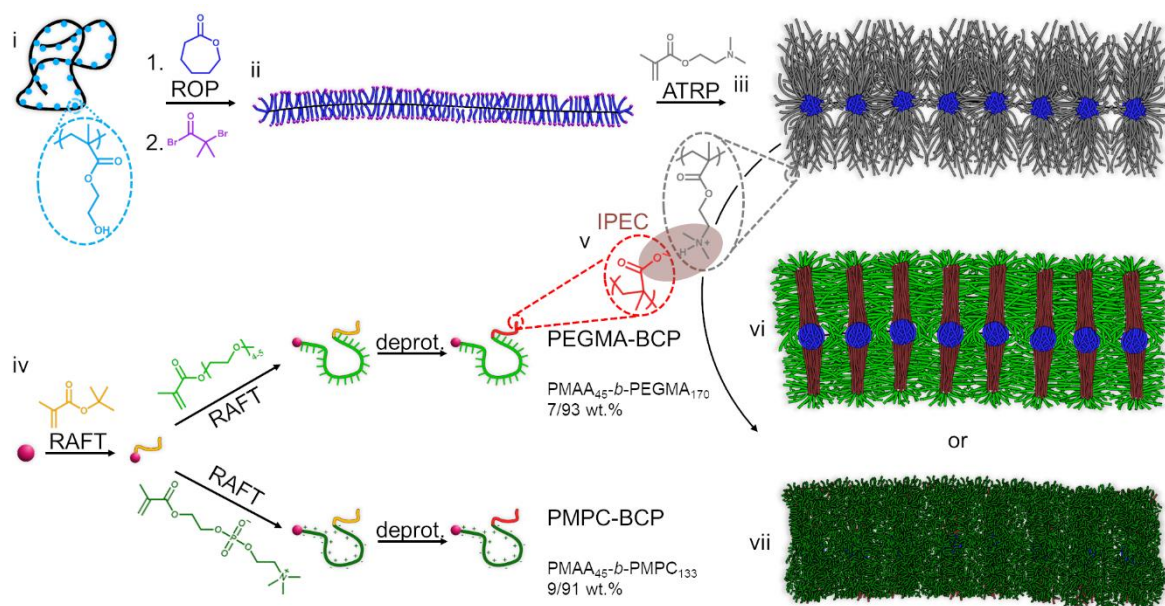
The nano-engineering of polymer particles has significantly progressed in recent years. In particular, bottom-up strategies based on self-assembly or template chemistry have enabled the fabrication of polymer particles across various length scales and geometries.^[1, 2] They have also allowed for introducing compartmentalisation into internal domains or specific functionalities.^[3-5] The potential applications of such ‘designer particles’ span beyond macromolecular science and into other areas of chemistry,^[6] engineering^[7, 8] and biomedicine.^[9, 10] Most examples of block copolymer self-assembly in solution make use of the incompatibility of various blocks or polymer domains, which drives the controlled formation of well-defined assemblies or superstructures.^[11, 12]

A straightforward, yet less commonly used method, exploits oppositely charged polymers to drive the self-assembly process via so called interpolyelectrolyte complex (IPEC) formation.^[13] An IPEC forms when a polycation and polyanion are mixed, with the two oppositely charged polyelectrolytes undergoing an associative phase separation in water, which induces a polymer-dense ‘coacervate’ or ‘polyplex’ phase under the release of their counterions. The formed IPEC phase is liquid-like, and not entirely hydrophobic, but rather a largely dehydrated polyion complex.^[14] The concept of IPEC has mostly been used within the context of gene delivery^[15] and the layer-by-layer assembly of polymer particles^[16] and coatings.^[17]

Increasingly, IPEC approaches have been investigated as a functionalisation and surface modification tool. When formed on polyelectrolyte surfaces (*e.g.* polymer brushes^[18, 19] or grafted spheres^[20]), the collapsing IPEC domain introduced distinct features. The ability of IPEC formation to yield defined structures is even more pronounced when the complexing polymer is a diblock copolymer (DBCP), where only one block is charged (*i.e.* takes part in the complexation).^[21] The non-associating block permits the introduction of new functional groups and surface chemistry. Similarly, it can stabilise the collapsing IPEC and lead to phase separation of the associating and non-associating polymer regions to segregate into two distinct domains. In a recent perspective article, Granick *et al.*^[22] emphasised on this general concept and described the use of IPECs in combination with DBCPs as an emerging method to alter the morphology of polyelectrolyte surfaces more generally. The formation and prediction of the phase separation remain challenging and the topic of recent investigations using computational modelling.^[23] In recent years, experimental progress has been made to expand the characterisation of IPEC structures using cryogenic electron tomography,^[24] to apply IPEC-modified particles (*e.g.* in nanomedicine^[25]) and to study IPEC formation on various substrates.^[26, 27] We have recently been able to adapt the IPEC concept to form highly structured polymer nanowires^[28] using a high aspect ratio cylindrical soft template, namely a molecular polymer brush (MPB).^[29]

Formation of IPEC nanostructures, including ours, use DBCP that feature non-ionic water-soluble segments (*e.g.* poly(ethylene glycol), PEG) to minimise interference in the phase separation process. Although IPECs have been formed involving other charge-neutral polymers,^[30] we are not aware of reports which use a zwitterionic DBCP on substrates in this process. Zwitterionic polymers are exciting building blocks for IPEC formation and possess unique properties that have attracted immense interest in nanomedicine and bioengineering communities. Their high charge density but net neutral character provides polyzwitterions with a thick hydration layer, resulting in excellent biocompatibility.^[31] Zwitterionic homo- and copolymers have therefore been explored as alternatives to PEG-based materials for the fabrication of biocompatible nanoparticles,^[32] antifouling surfaces^[33, 34] as well as drug-delivery nanocarriers.^[35]

Herein, we designed a molecular polymer brush template featuring a hydrophobic core and positively charged outer shell via a combination of controlled polymerisation techniques. Additionally, we produced two DBCPs with both negatively charged and charge-neutral segments. As the charge-neutral block we selected non-ionic poly[poly(ethylene glycol) methyl ether methacrylate] (PEGMA) or zwitterionic poly(2-methacryloyloxyethyl phosphorylcholine) (PMPC). Upon addition of either DBCP to the brush template, positively and negatively charged moieties complex to form IPECs within the brush shell (**Scheme 1**); switching the brush surface charge from positive to charge-neutral. A distinct difference in morphology was observed when the IPEC was formed using the zwitterionic DBCP, yet the phosphorylcholine-based copolymer was still able to establish well-defined, high aspect ratio, zwitterionic nano-cylinders.



Scheme 1. Formation of interpolyelectrolyte complexes on a MPB template

Utilisation of a high molecular weight polyinitiator backbone (i) to produce a precursor brush (ii) and subsequently a water-dispersible core-shell brush template (iii). Diblock copolymers of various compositions were produced using reversible-deactivation radical polymerisation (iv) before complexation with the template brush (v) to yield charge-neutral polymer nano-cylinders with regular compartmentalisation (vi) or a homogenous polyzwitterionic shell (vii).

Results and Discussion

We synthesised a core-shell MPB template using a combination of ring-opening polymerisation and atom-transfer radical polymerisation (ATRP, **Scheme S1**). First, a poly(ϵ -caprolactone) (PCL) core was grafted from a high-molecular weight poly(2-hydroxyethyl methacrylate) (PHEMA₇₅₀₀) polyinitiator backbone before modification of the terminal hydroxyl groups with α -bromoisobutyryl bromide to install ATRP initiating sites and yield a brush precursor (PHEMA₇₅₀₀-g-PCL₁₄-Br).^[36] The chemical structure of the MPB was confirmed via ¹H-NMR spectroscopy (**Figure S2**), which was further used to determine the PCL side chain length (using a previously reported grafting efficiency^[37]) and the chain-end modification. The PCL side chains were chain-extended with 2-(dimethylamino)ethyl methacrylate (DMAEMA) to yield a core-shell MPB (PHEMA₇₅₀₀-g-[PCL₁₄-b-PDMAEMA₁₆₆]). ¹H-NMR spectroscopy was used to monitor the monomer conversion, to verify the chemical composition of the final polymer architecture, as well as to calculate the degree of polymerisation of PDMAEMA (using a previously determined grafting efficiency^[36]).

The morphology of the core-shell brush was studied by atomic force microscopy (AFM), confirming the unimolecular and worm-like character of the brush template (**Figure S3-1**). The PDMAEMA shell permits the dispersion of the core-shell brush in aqueous media (pK_a PDMAEMA ≈ 7.0 ^[38]). AFM measurements on the protonated template brush (dispersed in sodium acetate buffer, NaOAc, 20 mM, pH 5.5) confirmed that the brushes preserved their worm-like architecture. Interestingly, AFM further indicated an undulated topography attributed to the compartmentalisation of the PCL core in aqueous environments (**Figure 1A** and **Figure S3-2**). This compartmentalisation is only slightly noticeable in AFM, however much more evident in cryo-TEM analyses, where the same brush revealed the formation of a distinct pearl-necklace structure. We had observed such surface minimisation of a PCL core in MPBs before,^[28, 39] where only the collapsed hydrophobic PCL core is resolved, while the solvated PDMAEMA shell remains concealed (**Figure 1B** and **Figure S4**). Statistical (**Figure**

S4C) and grey-scale (**Figure 1C**) analyses on the cryo-TEM images highlighted the high uniformity of the pearl-necklace structure, with a mean “pearl” diameter of $p_d = 13.1 \pm 2.3$ nm and regular “pearl-to-pearl” spacing of $p-p^\# = 8.3 \pm 3.2$ nm.

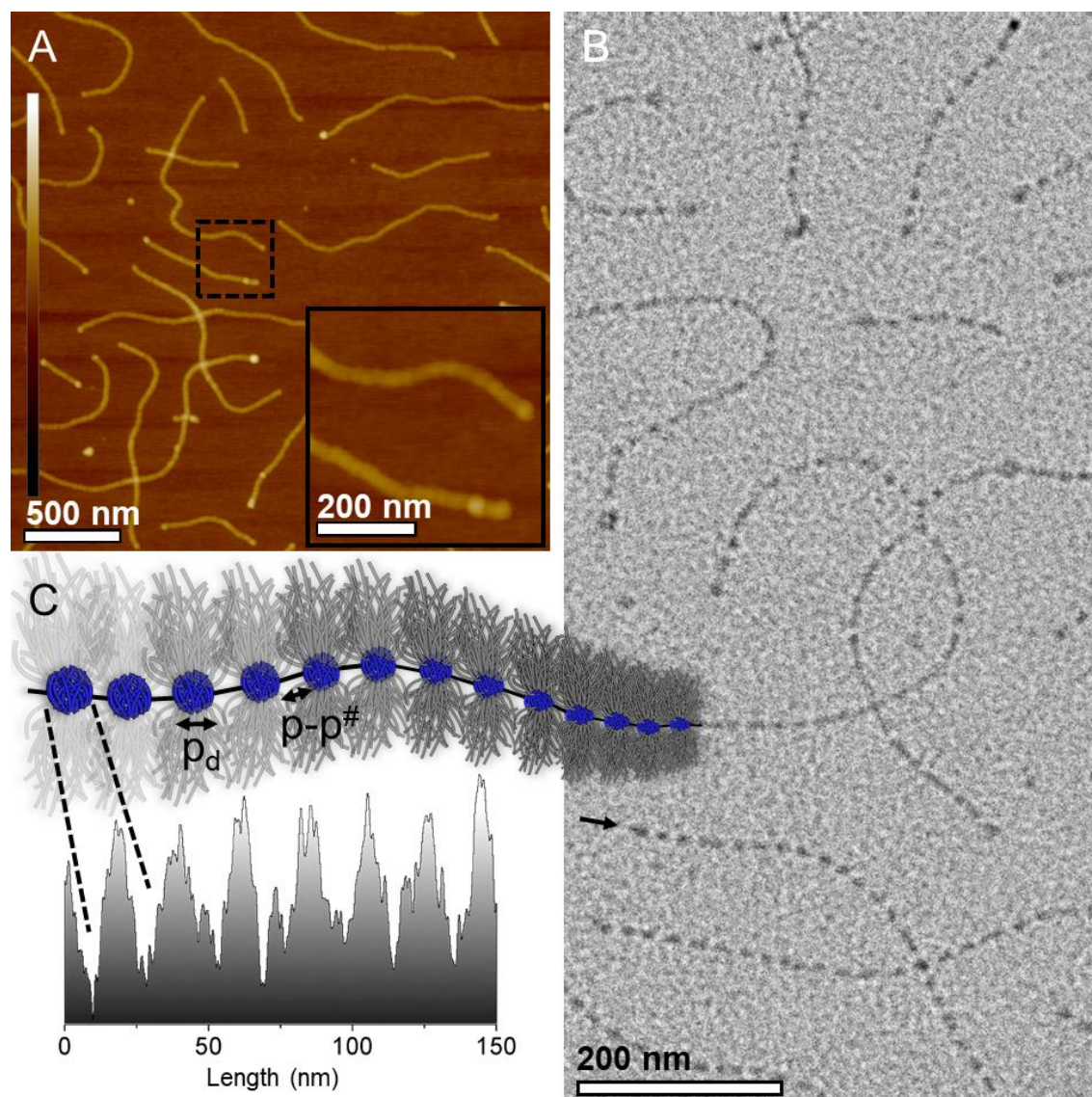


Figure 1. Characterisation of the core-shell brush. (A) AFM height image of the brush spin-coated from buffer solution onto freshly cleaved mica. z -scale is ± 20 nm. (B) Cryo-TEM image of the template dispersed in buffer. (C) Grey-scale analysis and schematic representation of the pearl-necklace structure (black arrow in image (B)).

Next, we produced DBCPs, each containing a negatively charged and a charge-neutral block. Poly(methacrylic acid) (PMAA) was selected as the negatively charged segment, to allow for complexation with the PDMAEMA shell of the template brush. As for the charge-neutral segment, we selected either a non-ionic PEGMA or zwitterionic PMPC. Both DBCPs were synthesised via reversible addition-fragmentation chain-transfer (RAFT) polymerisation (**Scheme S1**), starting with the synthesis of poly(*tert*-butyl methacrylate) (PtBMA₄₅, M_n NMR = 6 700 Da, see **Figure S5-1** for ¹H-NMR spectrum and end-group analysis). Size exclusion chromatography (SEC, **Figure S5-2**) was used to verify the molecular weight distribution of the macro-RAFT agent ($\mathcal{D} = 1.12$), including the subsequent chain-extension with PEGMA to yield PtBMA₄₅-*b*-PEGMA₁₇₀ ($\mathcal{D} = 1.24$). The chain-extension using MPC was performed analogously to PEGMA and ¹H-NMR spectroscopy was used to determine the chain length through conversion analysis and verify the polymer composition (**Figure S6-1**). Due to its

insolubility in the SEC solvent (*N,N*-dimethylacetamide), *Pt*BMA₄₅-*b*-PMPC₁₃₃ was analysed via aqueous SEC after a deprotection step (**Figure S6-2**). We aimed at a comparable weight ratio of negative to charge-neutral segments and the *tert*-butyl protective groups were subsequently removed in acidic conditions to expose the methacrylic acid (MAA) units and yield bishydrophilic charge-neutral DBCPs, namely PMAA₄₅-*b*-PEGMA₁₇₀ (PEGMA-DBCP, 55 100 Da, $f_{\text{MAA}} = 7$ wt.%) and PMAA₄₅-*b*-PMPC₁₃₃ (PMCP-DBCP, 43 400 Da, $\bar{D} = 1.35$, $f_{\text{MAA}} = 9$ wt.%). Both DBCPs were now water-soluble, enabling them to be mixed with the template brush to study the IPEC formation.

We dispersed the core-shell template brush in pH 5.5 buffer (NaOAc, 20 mM) to study the IPEC-driven self-assembly between the positively charged brush shell (pK_a PDMAEMA ≈ 7.0 ^[38]) and the negatively charged PMAA segments of the DBCP (pK_a PMAA ≈ 4.8 - 5.5 ^[40-42]). We first sought to study the PEGMA system, as we had previously demonstrated that PEO/PEGMA-based DBCPs carrying a quaternised polycation segment can be used to complex onto negatively charged MPB.^[28] A solution of PEGMA-DBCP ($c = 5$ g·L⁻¹) was added to a dispersion of the template brush ($c = 0.2$ g·L⁻¹) under gentle stirring to form PEGMA-IPEC. Nominally stoichiometric ratios were used to aim at compensating opposite charges, meaning that approximately five polymer chains of PEGMA-DBCP would need complex to one brush side chain to achieve charge neutrality (see **Supporting Information** for details of the calculation). Cryo-TEM evidenced the formation of internal IPEC morphologies, oriented perpendicularly to the primary axis of the brush template (**Figure 2A**). These internal features appear darker due to the largely dehydrated nature of the complexed DMAEMA/MAA domains and their higher electron density. The hydrophobic IPEC compartments are sandwiched between water-swollen, yet unresolved, PEGMA domains that aid the minimisation of unfavourable IPEC/water interfaces. Calculation of the internal IPEC volume ($\text{VOL}_{\text{PEGMA-IPEC}} \approx 39$ - 47 vol.%) suggests a parallel disc-like arrangement following classic theory of block copolymers.^[43] We postulate that the use of the template with collapsed hydrophobic core may contribute to the alternating arrangement between the IPEC and PEGMA domains; further investigation on this phenomenon is ongoing. In-depth grey-scale (**Figure 2B**) and statistical (**Figure 2C**) analyses of the IPEC morphology revealed a distinct uniformity within the internal feature diameters (f_d PEGMA-IPEC = 81.7 ± 7.9 nm), thicknesses (f_t PEGMA-IPEC = 8.9 ± 1.2 nm), as well as in their spacing (f_s PEGMA-IPEC = 13.7 ± 3.3 nm). Additionally, AFM analyses confirmed that the IPEC has successfully formed and altered the template brush (**Figure S7**).

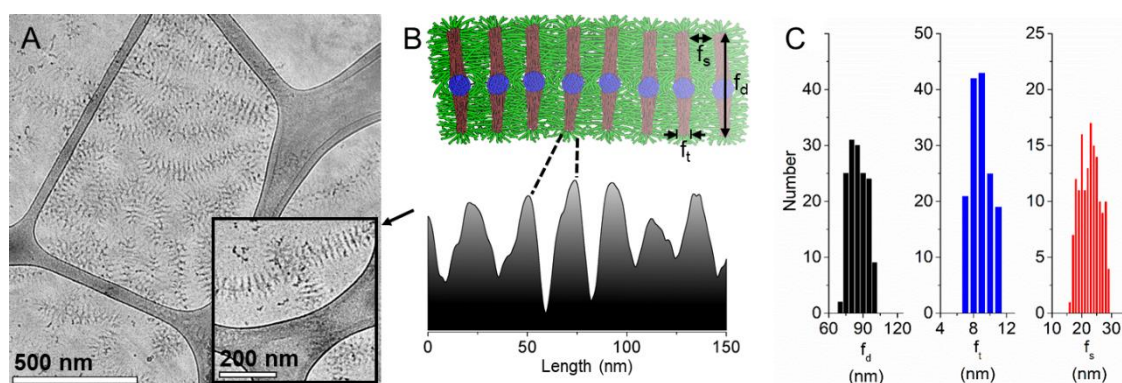


Figure 2. (A) Cryo-TEM images of PEGMA-IPEC formed upon electrostatic complexation between the brush template and the charge-neutral PEGMA-DBCP in pH 5.5 buffer. (B) Grey-scale analysis extracted from one specimen (black arrow in (A)) and schematic representation of the structured morphology. (C) Statistical analyses of the features diameter (f_d), features thickness (f_t) and feature-to-feature spacing (f_s) extracted from 150 discs in multiple cryo-TEM images.

We then added a solution of zwitterionic PMPC-DBCP ($c = 5$ g·L⁻¹) to a brush dispersion ($c = 0.2$ g·L⁻¹) under gentle stirring to assemble the PMPC-IPEC. Again, nominally

stoichiometric ratios were used to compensate all charges, meaning that approximately five polymer chains of PMPC-DBCP are required to complex onto one PDMAEMA side chain to achieve charge neutrality. Cryo-TEM measurements (**Figure 3A-C** and **Figure S8**) revealed a distinctly different morphology, indicating a dense brush-like shell compared to the highly regular internal structure of PEGMA-IPEC. Moreover, the large diameter of the cylindrical zwitterionic nano-cylinders featuring PMPC-IPEC ($f_d \text{ PMPC-IPEC} = 154 \pm 3 \text{ nm}$) compared to the previously unresolved PDMAEMA template shell demonstrates successful IPEC formation and surface modification. We expect that the zwitterionic nature (and high ionic strength) of the DBCP interferes with the electrostatic complexation mechanism and prevents the formation of distinct IPEC domains, which in turn prevents phase-separation. AFM images and cross-sectional analyses (**Figure 3D** and **Figure S9**) further supported the successful complexation of the DBCP onto the template brush, displaying a large increase of the feature height ($h_{\text{PMPC-IPEC}} \approx 10\text{-}12 \text{ nm}$ vs. $h_{\text{template}} \approx 4 \text{ nm}$). Note, the difference in brush diameter and brush height in general is attributed to the brushes spreading and flattening upon drying.

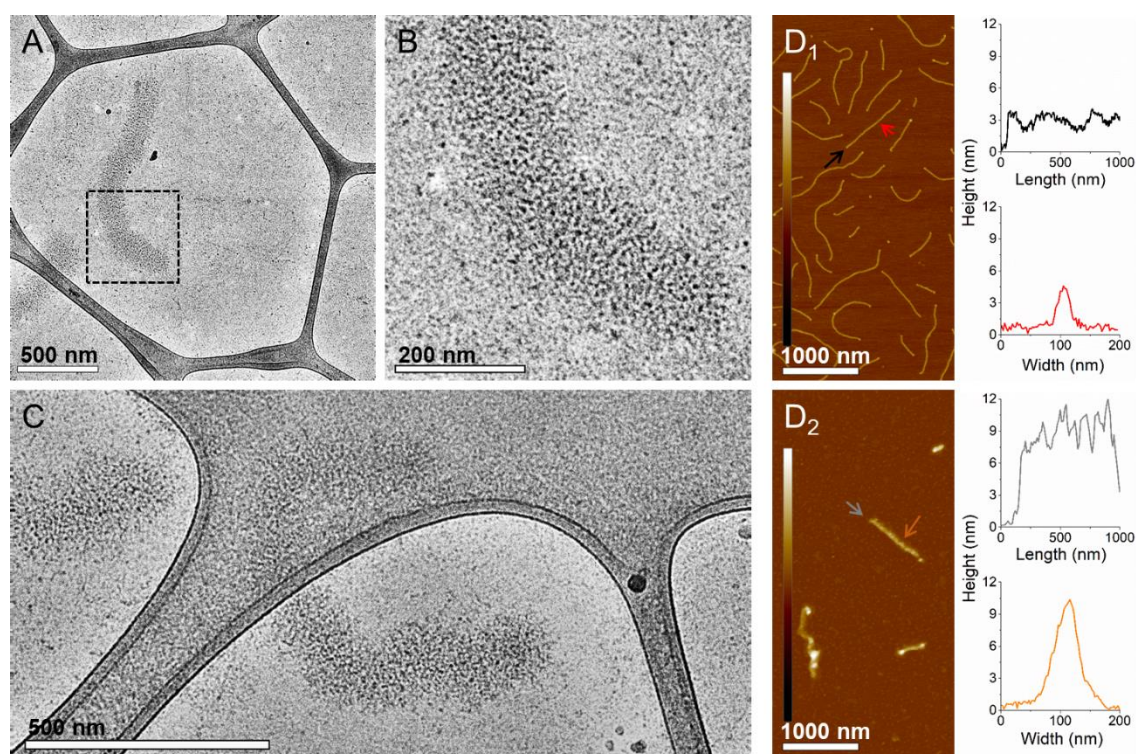


Figure 3. (A-C) Cryo-TEM images of the nanostructures formed upon electrostatic complexation of the core-shell brush and the zwitterionic PMPC-DBCP (PMPC-IPEC). (D) AFM height images and cross-sectional analyses of the pristine template (D₁) and PMPC-IPEC (D₂). z -scale is $\pm 40 \text{ nm}$.

ξ -potential measurements (**Figure S10**) confirmed the successful complexation (*i.e.* the surface modification via IPEC formation), evidenced by the shift of the potential towards neutral values upon addition of PMPC-DBCP onto the polycationic template ($\xi_{\text{template}} = + 32.6 \text{ mV}$). However, seemingly a 1:1 molar ratio of template DMAEMA to MAA units was not enough to achieve full charge neutralisation ($\xi_{\text{PMPC-IPEC 1:1}} = + 23.3 \text{ mV}$) and a charge-neutral complex was obtained only after the addition of a large excess of DBCP ($\xi_{\text{PMPC-IPEC 1:5}} = + 2.9 \text{ mV}$). It is possible that the complexation cannot be completed when stoichiometric amounts of DBCP are introduced into the mixture, due to the inaccessibility of all positive charges or incomplete deprotonation of the PMAA segments given that the assembly proceeded at pH close to that of the pK_a of the PMAA block. Therefore, an excess of DBCP was required to drive the complexation towards neutralisation under these conditions. To gain further insight, we performed an isothermal titration calorimetry (ITC) study to assess the binding of the

deprotonated PMAA segment of the PMPC-DBCP onto the protonated PDMAEMA shell. ITC monitors incremental enthalpies of interaction between binding partners during a titration experiment. The technique is commonly used to study the association of proteins with other molecules, yet few examples exist where ITC has been used to evidence the formation of IPECs.^[44] A PMPC-DBCP solution at 491 mM (*i.e.* 18.7 mM $-\text{COO}^-$) was titrated into a solution of MPB at 1.0 nM (*i.e.* 1.245 mM $-\text{NH}(\text{CH}_3)_2^+$). The release of heat as a function of time was monitored by ITC during the complexation (upper panels in **Figure S11**). The formation of a sharp negative peak after each PMPC-DBCP injection indicates an exothermic complexation, while the decrease in the heat generated in subsequent injections indicates the progressive neutralisation of the DMAEMA positive charges. The binding isotherm curve fitted to the thermogram (bottom panels in **Figure S11**) revealed an apparent association constant K_a of $5.25 \pm 0.61 \times 10^3 \text{ M}^{-1}$ with a binding stoichiometry $n = 1.87$. This binding stoichiometry suggests that almost two MAA units must be supplied to each DMAEMA unit to ensure complexation. This deviation in stoichiometry can be explained by the pH of the aqueous medium being close to the $\text{p}K_a$ of PMAA, which prevents the full deprotonation of the methacrylic acid groups. We can nonetheless observe that the IPEC formation is thermodynamically favourable ($\Delta G = -5.07 \text{ kcal}\cdot\text{mol}^{-1}$). The enthalpic contribution to binding ($\Delta H = -0.336 \pm 0.010 \text{ kcal}\cdot\text{mol}^{-1}$) is rather small, yet still favourable. The thermodynamic driving force for association between the two IPEC components arises primarily through the favourable entropy of association ($\Delta S = 15.9 \text{ cal}\cdot\text{mol}^{-1}\cdot\text{K}^{-1}$), a factor which is likely to be a consequence of expulsion of water and counterions during complexation. This demonstrates the successful alteration of the surface chemistry of the template and efficient formation of cylindrical zwitterionic nanoparticles.

Conclusion

In summary, we demonstrated that the IPEC structuring approach using zwitterionic components is feasible. We used MPBs and DBCPs to construct tailor-made cylindrical polymer particles, where the MPB template dictates the overall 1D structure of the forming material and the IPEC formation induces the morphological changes to the interior and/or the periphery of the template. When the IPEC is formed by a charge-neutral PEGMA-DBCP, a well-defined caterpillar-like internal morphology developed. This originated from the stabilisation of the forming, hydrophobic IPEC domain by the non-ionic hydrophilic PEGMA. On the contrary, the use of a polyzwitterionic-based PMPC-DBCP led to a dense covering of the template without visibly introducing an internal morphology. The zwitterionic character prevented a phase-separation, commonly seen by non-ionic charge-neutral DBCPs. This may stem from weak interaction between zwitterions and the charged template brush shell or the fact that the zwitterions overall weaken the IPEC itself. However, IPEC formation was possible and further research is underway to use such zwitterionic polymer cylinders in cartilage mimetic materials, as their observed structure closely resembled the structure of proteoglycan aggregates,^[45, 46] *i.e.* nature's brush architectures commonly found in cartilage.

Supporting Information

Supporting Information including materials and methods, polymer synthesis and characterisation as well as general protocols for the formation of IPEC structures is available from the Wiley Online Library or from the author.

(<https://onlinelibrary.wiley.com/doi/full/10.1002/marc.202000401>)

Acknowledgements

The authors thank A/Prof. Chiara Neto for providing access to atomic force microscopes and the Key Centre for Polymers and Colloids (KCPC) for access to equipment. T.P. acknowledges

The University of Sydney Nano Institute (Sydney Nano) for a Postgraduate Top-Up Scholarship. N. thanks the Academy of Finland's Centre of Excellence in Molecular Engineering of Biosynthetic Hybrid Materials (HYBER, 2014-2019) and the Aalto University Nanomicroscopy Centre. C.S.M. was a grateful recipient of a Marie Skłodowska-Curie Global Fellowship, receiving funding from the European Union's Horizon 2020 research and innovation programme under the Marie Skłodowska-Curie grant agreement No 702927, and thanks Prof. Gideon Davies (University of York) for access to the isothermal titration calorimeter. M.M. acknowledges the Australian Research Council (DE180100007) for funding this project.

References

- [1] F. H. Schacher, P. A. Rugar, I. Manners, *Angew. Chem. Int. Ed.* **2012**, *51*, 7898.
- [2] J.-F. Lutz, J.-M. Lehn, E. W. Meijer, K. Matyjaszewski, *Nat Rev Mater* **2016**, *1*, 16024.
- [3] R. Fleet, E. Dungen (van den), T. A., B. Klumperman, *S. Afr. J. Sci.* **2011**, *107*, 424.
- [4] C. K. Wong, X. Qiang, A. H. E. Müller, A. H. Gröschel, *Prog Polym Sci* **2020**, 101211.
- [5] T. Pelras, C. S. Mahon, M. Müllner, *Angew. Chem. Int. Ed.* **2018**, *57*, 6982.
- [6] A. H. Gröschel, A. H. E. Müller, *Nanoscale* **2015**, *7*, 11841.
- [7] A. Steinhaus, T. Pelras, R. Chakroun, A. H. Gröschel, M. Müllner, *Macromol. Rapid Commun.* **2018**, *39*, 1800177.
- [8] D.-P. Song, T. H. Zhao, G. Guidetti, S. Vignolini, R. M. Parker, *ACS Nano* **2019**, *13*, 1764.
- [9] A. K. Pearce, R. K. O'Reilly, *Bioconjugate Chem.* **2019**, *30*, 2300.
- [10] C. K. Wong, F. Chen, A. Walther, M. H. Stenzel, *Angew. Chem. Int. Ed.* **2019**, *58*, 7335.
- [11] F. D'Agosto, J. Rieger, M. Lansalot, *Angew. Chem. Int. Ed.* **2020**, *59*, 8368.
- [12] J.-F. Lutz, *Polymer Int.* **2006**, *55*, 979.
- [13] D. V. Pergushov, A. H. E. Müller, F. H. Schacher, *Chem. Soc. Rev.* **2012**, *41*, 6888.
- [14] D. V. Pergushov, E. V. Remizova, J. Feldthussen, A. B. Zezin, A. H. E. Müller, V. A. Kabanov, *J. Phys. Chem. B* **2003**, *107*, 8093.
- [15] B. S. Kim, S. Chuanoi, T. Suma, Y. Anraku, K. Hayashi, M. Naito, H. J. Kim, I. C. Kwon, K. Miyata, A. Kishimura, K. Kataoka, *J. Am. Chem. Soc.* **2019**, *141*, 3699.
- [16] J. Cui, M. P. van Koeveden, M. Müllner, K. Kempe, F. Caruso, *Adv. Colloid Interfac.* **2014**, *207*, 14.
- [17] A. M. C. Maan, A. H. Hofman, W. M. de Vos, M. Kamperman, *Adv Funct Mater* **2020**, 2000936.
- [18] S. V. Larin, D. V. Pergushov, Y. Xu, A. A. Darinskii, A. B. Zezin, A. H. E. Müller, O. V. Borisov, *Soft Matter* **2009**, *5*, 4938.
- [19] Y. Xu, O. V. Borisov, M. Ballauff, A. H. E. Müller, *Langmuir* **2010**, *26*, 6919.
- [20] F. Schacher, E. Betthausen, A. Walther, H. Schmalz, D. V. Pergushov, A. H. E. Müller, *ACS Nano* **2009**, *3*, 2095.
- [21] A. Harada, K. Kataoka, *Polym. J.* **2018**, *50*, 95.
- [22] B. Tsang, C. Yu, S. Granick, *ACS Nano* **2014**, *8*, 11030.
- [23] G. M. C. Ong, C. E. Sing, *Soft Matter* **2019**, *15*, 5116.
- [24] T. I. Löbbling, J. S. Haataja, C. V. Synatschke, F. H. Schacher, M. Müller, A. Hanisch, A. H. Gröschel, A. H. E. Müller, *ACS Nano* **2014**, *8*, 11330.
- [25] C. V. Synatschke, T. Nomoto, H. Cabral, M. Förtsch, K. Toh, Y. Matsumoto, K. Miyazaki, A. Hanisch, F. H. Schacher, A. Kishimura, N. Nishiyama, A. H. E. Müller, K. Kataoka, *ACS Nano* **2014**, *8*, 1161.

- [26] J.-M. Malho, M. Morits, T. I. Löbbling, Nonappa, J. Majoinen, F. H. Schacher, O. Ikkala, A. H. Gröschel, *ACS Macro Lett.* **2016**, *5*, 1185.
- [27] F. H. Schacher, T. Rudolph, M. Drechsler, A. H. E. Müller, *Nanoscale* **2011**, *3*, 288.
- [28] T. Pelras, C. S. Mahon, Nonappa, O. Ikkala, A. H. Gröschel, M. Müllner, *J. Am. Chem. Soc.* **2018**, *140*, 12736.
- [29] M. Müllner, A. H. E. Müller, *Polymer* **2016**, *98*, 389.
- [30] M. Cai, Y. Ding, L. Wang, L. Huang, X. Lu, Y. Cai, *ACS Macro Lett.* **2018**, *7*, 208.
- [31] L. D. Blackman, P. A. Gunatillake, P. Cass, K. E. S. Locock, *Chem. Soc. Rev.* **2019**, *48*, 757.
- [32] J. Wang, S. Yuan, Y. Zhang, W. Wu, Y. Hu, X. Jiang, *Biomater. Sci.* **2016**, *4*, 1351.
- [33] S. Kalasin, R. A. Letteri, T. Emrick, M. M. Santore, *Langmuir* **2017**, *33*, 13708.
- [34] Q. Liu, W. Li, H. Wang, B.-m. Z. Newby, F. Cheng, L. Liu, *Langmuir* **2016**, *32*, 7866.
- [35] T. Goda, K. Ishihara, Y. Miyahara, *J. Appl. Polym. Sci.* **2015**, *132*, 41766.
- [36] M. Müllner, T. Lunkenbein, J. Breu, F. Caruso, A. H. E. Müller, *Chem Mater* **2012**, *24*, 1802.
- [37] S. Y. Yu-Su, S. S. Sheiko, H.-i. Lee, W. Jakubowski, A. Nese, K. Matyjaszewski, D. Anokhin, D. A. Ivanov, *Macromolecules* **2009**, *42*, 9008.
- [38] V. Bütün, S. P. Armes, N. C. Billingham, *Polymer* **2001**, *42*, 5993.
- [39] M. Müllner, T. Lunkenbein, M. Schieder, A. H. Gröschel, N. Miyajima, M. Förtsch, J. Breu, F. Caruso, A. H. E. Müller, *Macromolecules* **2012**, *45*, 6981.
- [40] S. Dai, P. Ravi, K. C. Tam, B. W. Mao, L. H. Gan, *Langmuir* **2003**, *19*, 5175.
- [41] J. Zhang, N. A. Peppas, *Macromolecules* **2000**, *33*, 102.
- [42] T. A. Sonia, C. P. Sharma, "6 - Polymers in oral insulin delivery", in *Oral Delivery of Insulin*, T.A. Sonia and C.P. Sharma, Eds., Woodhead Publishing, 2014, p. 257.
- [43] M. W. Matsen, F. S. Bates, *Macromolecules* **1996**, *29*, 1091.
- [44] S. Bharadwaj, R. Montazeri, D. T. Haynie, *Langmuir* **2006**, *22*, 6093.
- [45] H.-Y. Lee, L. Han, P. J. Roughley, A. J. Grodzinsky, C. Ortiz, *J. Struct. Biol.* **2013**, *181*, 264.
- [46] T. B. Goudoulas, E. G. Kastrinakis, S. G. Nychas, L. G. Papazoglou, G. M. Kazakos, P. V. Kosmas, *Ann. Biomed. Eng.* **2010**, *38*, 57.